

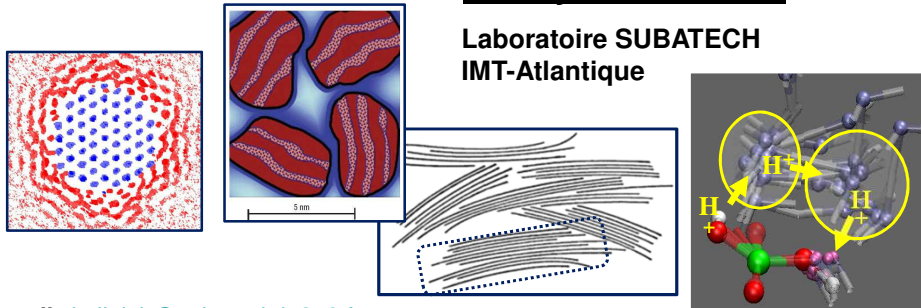
NE-M1-PRI12ENP – Integrated Nuclear Engineering Project

Molecular Modeling of Materials for Nuclear Waste Disposal Applications

Lecture 8 - Quantum MD, other advanced simulation techniques, future challenges

Andrey G. Kalinichev

Laboratoire SUBATECH
IMT-Atlantique



E-mail: kalinich@subatech.in2p3.fr

<https://www.imt-atlantique.fr/en/person/andrey-kalinichev>



NE-M1-PRI12ENP – Integrated Nuclear Engineering Project, February-June 2025
"Molecular modeling of materials for nuclear waste disposal applications"

1

Advanced Molecular Simulation Techniques

- Non-equilibrium MD
- External electric fields
- Crystallization of water and melting of ice
- Shock wave propagation in materials
- Radiation damage
- Plasticity of materials
- Ab initio (quantum) MD
- "Reactive" force fields and simulations
- Multiscale approaches



NE-M1-PRI12ENP – Integrated Nuclear Engineering Project, February-June 2025
"Molecular modeling of materials for nuclear waste disposal applications"

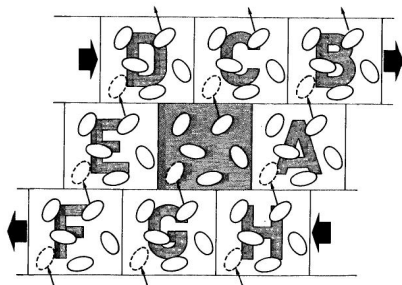
2

Non-Equilibrium Molecular Dynamics (NEMD)

$$\dot{\mathbf{q}} = \mathbf{p}/m + \mathcal{A}_p \cdot \mathcal{F}(t)$$

$$\dot{\mathbf{p}} = \mathbf{f} - \mathcal{A}_q \cdot \mathcal{F}(t)$$

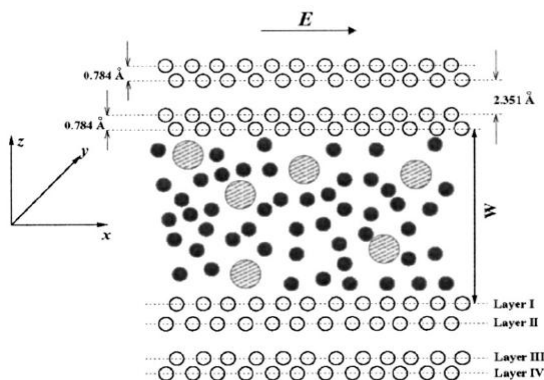
Homogeneous shear
boundary conditions



- A perturbation (external field) is introduced into equations of motion
- The quantities $\mathcal{A}_p(q, p)$ and $\mathcal{A}_q(q, p)$ describe the way in which the field couples to the molecules
- In standard linear response theory, the perturbation is represented as an additional term in the system Hamiltonian
- When a perturbation is applied in MD simulation, the system typically heats up. This heating may be controlled by techniques analogous to *NVT* and *NPT* algorithms (thermostats, barostats)

Ion Concentrations and Velocity Profiles in Nanochannel Electroosmotic Flows

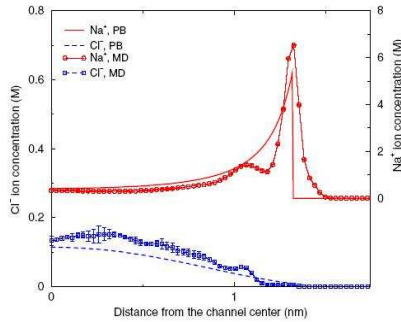
Qiao and Aluru (2003) *J.Chem.Phys.*, **118**, 4692-4701



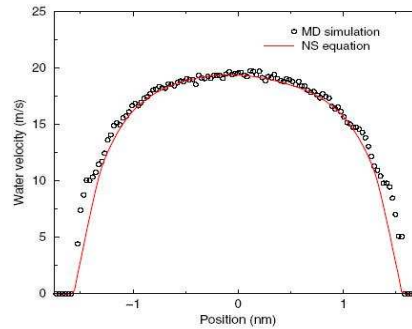
- The two channel walls are symmetrical with respect to the channel center line.
- Each wall is made up of four layers of silicon atoms.
- The channel width W is defined as the distance between the two innermost wall layers.
- The dark dots are H_2O molecules and the shaded circles are Cl^- or Na^+ ions.
- $z = 0$ corresponds to the central plane of the channel system.

Ion Concentrations and Velocity Profiles in Nanochannel Electroosmotic Flows

Qiao and Aluru (2003) *J.Chem.Phys.*, **118**, 4692-4701



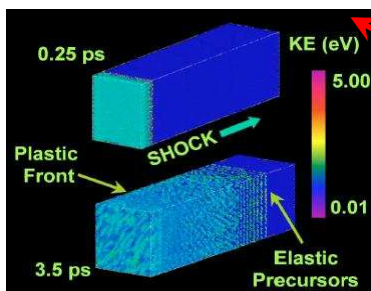
Na⁺ and Cl⁻ ion concentrations across the channel for case 2 ($W = 3.49$ nm, $\sigma_s = -0.130$ C/m²). The error bars are estimated from three continuous MD runs each of 4.2 ns long.



Comparison of water velocity profile across the channel for case 2 ($W = 3.49$ nm, $\sigma_s = -0.130$ C/m²) as predicted by the MD simulation and by the continuum flow theory.

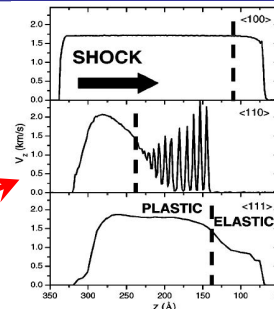
Atomistic Simulation of Shock Wave Propagation

Single-crystal copper: Bringa et al. (2004) *J.Appl.Phys.*, **96**, 3793-3799



- ◆ Snapshots of a shock along $\langle 110 \rangle$, showing the elastic precursors and the plastic wave
- ◆ Coloring proportional to the kinetic energy of the atoms
- ◆ The volume of the simulated sample was roughly $25a \times 25a \times 100a$, with $a = 3.615 \text{ \AA}$.

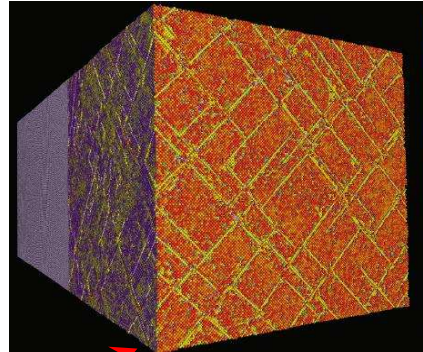
- ◆ Snapshots of velocity profiles for shock waves along $\langle 100 \rangle$, $\langle 110 \rangle$, and $\langle 111 \rangle$, taken 3 ps after the shock was started, for a piston pressure of 100 GPa
- ◆ Dashed lines give approximate location of plastic front



Plasticity Induced by Shock Waves in Nonequilibrium Molecular Dynamics Simulations

Holian and Lomdahl (1998) *Science*, **280**, 2085-2088

- ◆ NEMD simulations of shock waves in 3D FCC crystals with cross-sectional dimensions of 100 x 100 unit cells (10,000,000 atoms)
- ◆ The system slips along all of the available {111} slip planes, in different places along the nonplanar shock front
- ◆ For weaker shock waves (below the perfect-crystal yield strength), stacking faults can be nucleated by preexisting extended defects



Pattern of intersecting stacking faults at piston face (impact plane) induced by collision with momentum mirror at piston velocity $u_p/c_0 = 0.2$. Shock wave has advanced halfway to the rear (~250 planes). Atoms are colored according to potential energy (color bar at side, energy increasing from bottom).

Dislocation Nucleation in Shocked FCC Solids

100 x 100 x 200 FCC unit cells

Hatano (2004) *PRL*, **93**, 085501-1

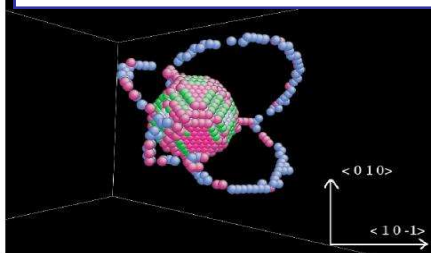


FIG. 2 (color online). Four partial dislocation loops nucleate on the void surface. Void radius is 2.4 nm and piston velocity is 70 m/s. Atoms of 12 nearest neighbors are not presented in order to see exclusively dislocations and void surface. Green, red, and blue atoms have 10, 11, and 13 nearest neighbors, respectively [15].

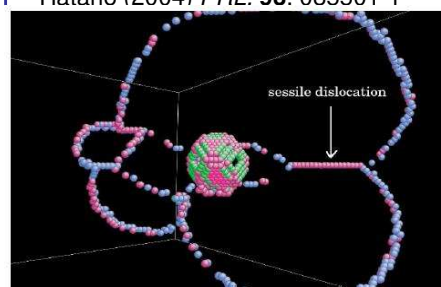


FIG. 3 (color online). Thirteen picoseconds after Fig. 2. Partial dislocation loops are extended and Lomer-Cottrell sessile dislocation is formed.

In a defective crystal with a void, dislocations are found to nucleate on the void surface. Hugoniot elastic limit (HEL) drastically decreases to 15% of the perfect crystal when the void radius is 3.4 nanometers (~10 times the size of the atoms). The decrease of HEL becomes larger as the void radius increases, but HEL becomes insensitive to temperature.

Crystallization of Liquid Water in MD Simulations

Svishchev & Kusalik (1994) *Phys.Rev.Lett*, **73**, 975-979

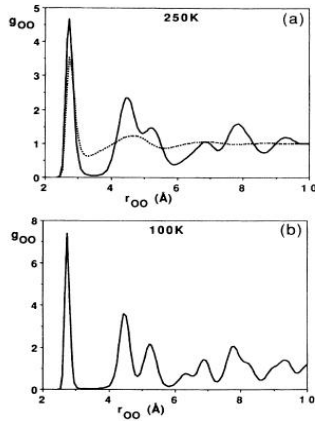


FIG. 1. The radial distribution functions of oxygen atoms in TIP4P water. (a) The supercooled liquid (dotted line) at 250 K with no applied field, and the polar ice (solid line) formed from this liquid at 250 K under the field of 0.5 V/Å. (b) Polar ice I at 100 K.

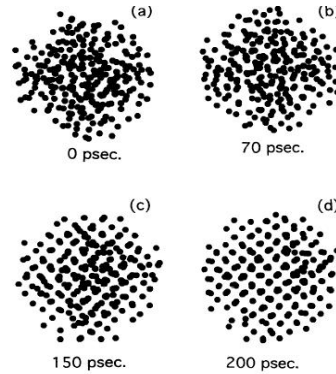
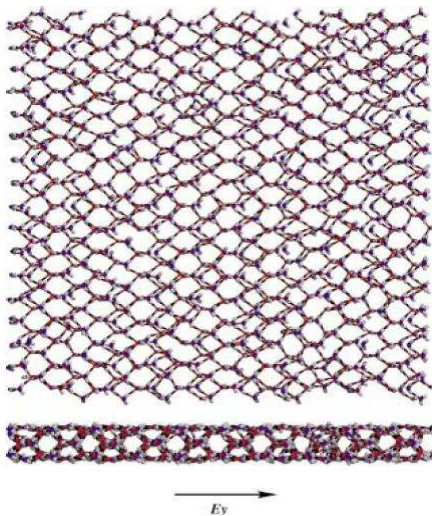


FIG. 3. Molecular configurations of a water system generated during a field-induced phase transition. (a) Initial liquid water configuration. (b), (c), and (d) Applied-field results at different stages of ice formation. The dots represent the oxygen atoms of the water molecules projected onto the x - y plane of the laboratory-fixed frame. The applied field is acting along the normal to the plane of the figure. All data are at 250 K for a field of 0.5 V/Å.

Electrofreezing of Confined Water

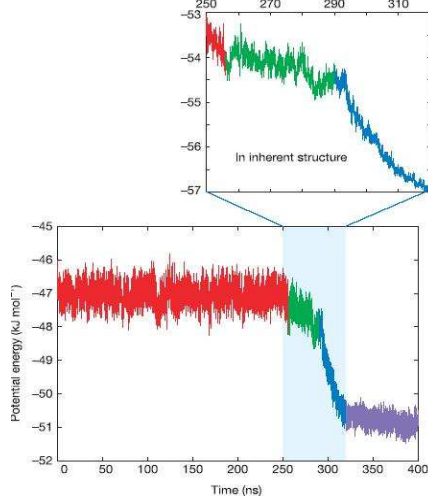
Zangi & Mark (2004) *J.Chem.Phys.*, **120**, 7123-7130



- ◆ Instantaneous configuration of the lateral and transverse structure of confined TIP5P ice.
- ◆ Oxygen atoms are depicted in blue, hydrogen atoms in gray, and the lone pair electron sites in red.
- ◆ $H = 0.92$ nm
- ◆ $A = 46.24$ nm²
- ◆ $T = 280$ K
- ◆ $E = 5$ V/nm along the y axis.
- ◆ "Due to the difficulty in observing spontaneous homogenous nucleation in molecular liquids on the time scale applicable to computational studies, the thermodynamic conditions that are used are more drastic than those that are used normally in experiments."

Slow Processes: Crystallization of Liquid Water in MD Simulations

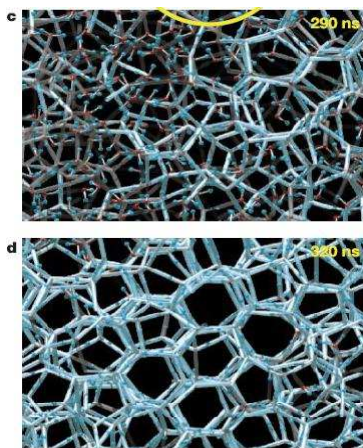
Matsumoto et al. (2002) *Nature*, **416**, 409-413



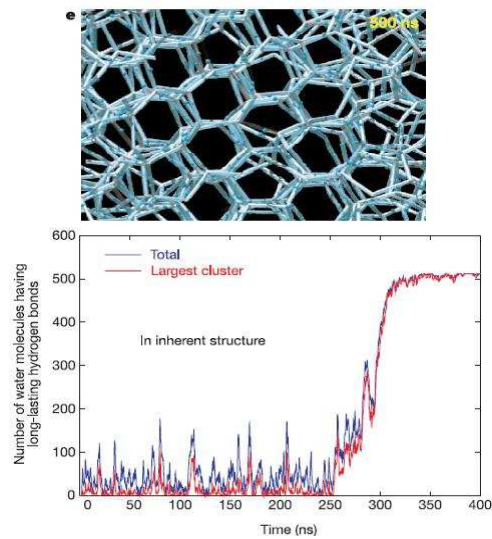
Potential energy of the instantaneous structures in the NVT MD trajectory for 512 TIP4P H₂O molecules after quenching from 400K to 230K (at $t = 0$).

- ◆ Cubic MD box with PBC
- ◆ The inset shows the total potential energies of the inherent structures, corresponding to the instantaneous structures in the trajectory for $t = 250$ – 320 ns. Inherent structures are calculated by local quenching at 10ps intervals.
- ◆ The freezing process can be divided into four stages:
 1. long quiescent period (red line)
 2. slow energy-decreasing period (green)
 3. fast energy-decreasing period (blue)
 4. crystallization-completion period (purple).

Slow Processes: Crystallization of Liquid Water in MD Simulations



Matsumoto et al. (2002) *Nature*, **416**, 409-413



Some More Challenges: Rare Events, Slow Processes

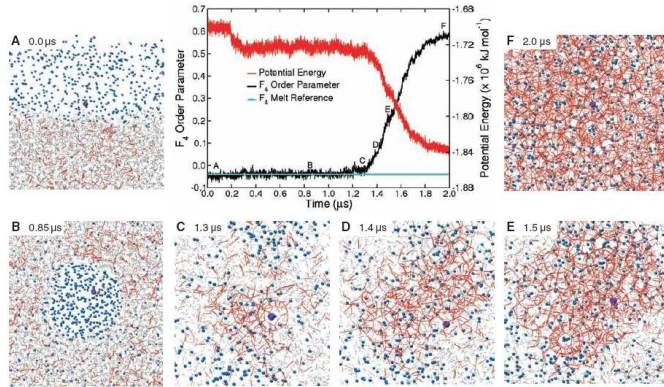
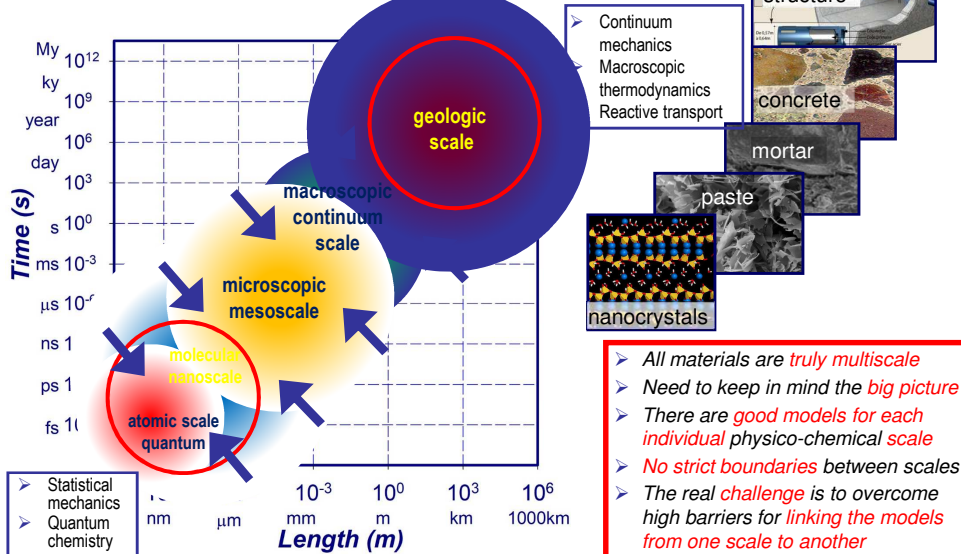


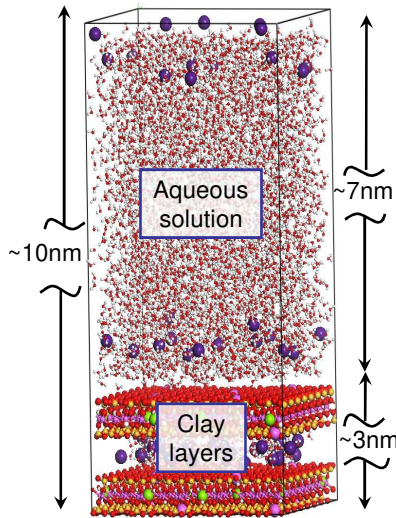
Fig. 1. Potential energy and F_4 order parameter for the methane-water system over the course of the simulation. A similar plot of the nucleation data and system snapshots for the 5- μ s trajectory is shown in fig. S1. The reference F_4 value (≈ 0.04) for a fully melted hydrate (horizontal blue line) helps to identify the beginning of nucleation at ≈ 1.2 μ s. Snapshots (A) through (F) show the system evolution during the simulation (images are only a portion of the periodic simulation box). Water is represented as gray lines, methane as blue spheres, and hydrogen bonds between water molecules as red lines. The larger violet sphere represents the first methane molecule to become permanently encathrated. During the time preceding nucleation, this methane molecule migrates from the vapor to the liquid and back several times. The water molecules are time-averaged over 2 ns to aid in the visualization. Movie S1 shows the complete nucleation trajectory. The methane concentration in the water phase and the gas density during the simulation are given in table S1.

- Methane clathrate formation from aqueous solution (Walsh et al., 2009)
- $\sim 10,000$ atom system; 2μ s simulation $\Rightarrow 2 \cdot 10^9$ time steps

Time and Length Scales of Geologic and Environmental Materials' Simulation



MD Modeling of Clay-Solution Interfaces



Classical Newtonian dynamics

- $N_{\text{tot}} \sim 3,000 - 10,000$ atoms
- $N_{\text{H}_2\text{O}} \sim 0 - 1,000$ molecules
- *ClayFF* force field (Cygan et al., 2004)
- $a \times b \times c \sim 3 \times 3 \times 10 \text{ nm}^3$
- Periodic boundary conditions
- *NVT*- or *NPT*-ensemble $T=300\text{K}$; $P=1 \text{ bar}$
- $t \sim 200 - 1,000 \text{ ps}$
- $\Delta t = 0.5-1.0 \text{ fs}$

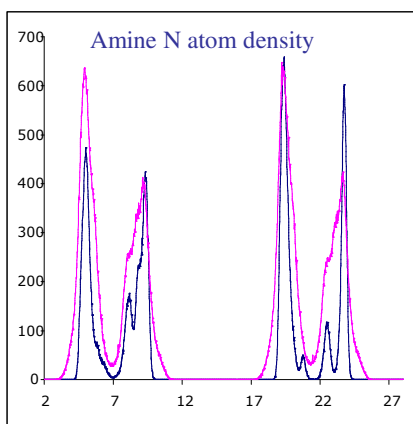
Solution structure:

- ✓ Atomic density profiles (\perp)
- ✓ Atomic density surface distributions (\parallel)
- ✓ Topology of the interfacial H-bond network

Dynamics:

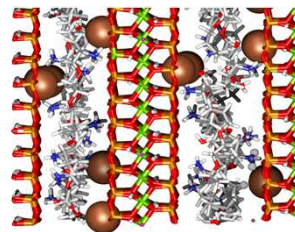
- ✓ Diffusion coefficients (longer time scale)
- ✓ Spectra of vibrational and rotational dynamics (shorter time scale)

Effects of Scale: Non-Swelling Amine-Clay Composites



- 7160 atom model
- 350,840 atom model

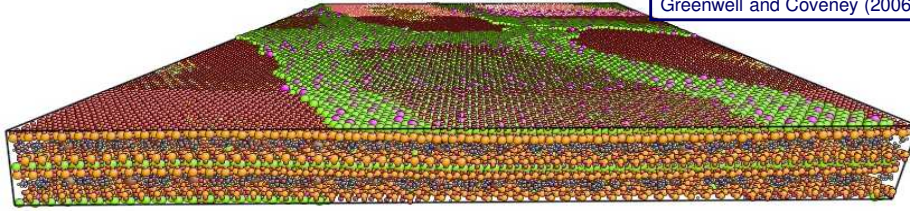
(Greewell and Coveney, 2006)



- The 1-D atomic density profile for the 350K atom model is much more diffuse
- "Increased sampling phase space" is a plausible explanation
- However, when the 350K atom model was *visualized* it became apparent that something else is happening

Large-Scale MD Case-Study: Sheet Undulations in Non-Swelling Amine-Clay Composites

Greenwell and Coveney (2006)



- Within very large simulation super-cells (350,840 atoms; 28nm × 50nm × 3nm) the clay sheets had been able to flex, resulting in a much broader distribution of atom density
- **Structural flexibility is even more important for larger systems**
- This distortion may be more evident at even larger super cell sizes, or using 2 -D boundary conditions
- Small and large model might have different and not obvious size effects, which can be beneficial or detrimental for the analysis
- It is hard to separate 1-D density profiles and 2-D surface density distribution for large systems

Langmuir

Article
pubs.acs.org/Langmuir

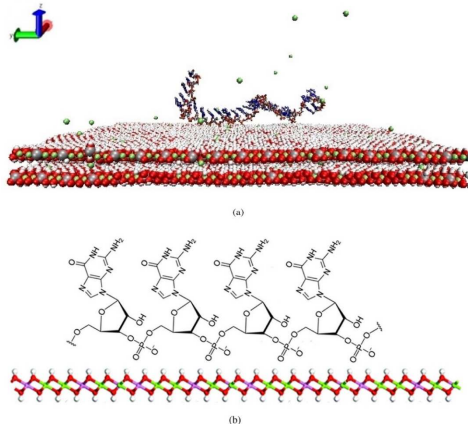
Influence of Surface Chemistry and Charge on Mineral–RNA Interactions

Jacob B. Swadling,[†] James L. Suter,[†] H. Christopher Greenwell,[‡] and Peter V. Coveney^{*†}

[†]The Centre for Computational Science, Department of Chemistry, University College London, 20 Gordon Street, London, WC1H 0AJ, United Kingdom

[‡]Department of Earth Sciences, South Road, Durham University, Durham, DH1 3LE, United Kingdom

Langmuir 2013, 29, 1573–1583



ARTICLE

DOI: 10.1038/s41467-017-02248-7

OPEN

Mineral surface chemistry control for origin of prebiotic peptides

Valentina Erastova¹, Matteo T. Degiacomi¹, Donald G. Fraser² & H. Chris Greenwell³

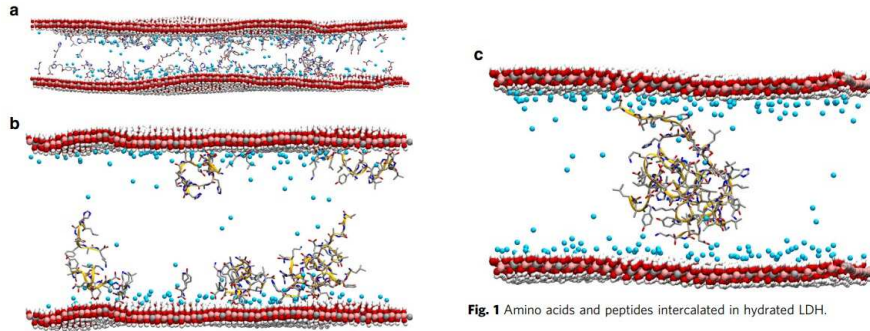
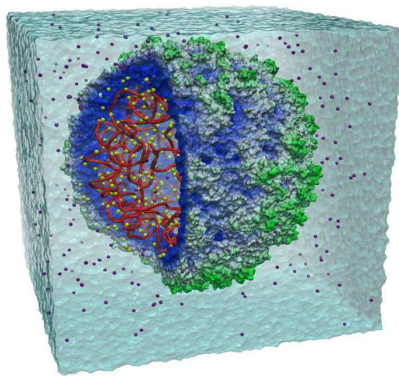


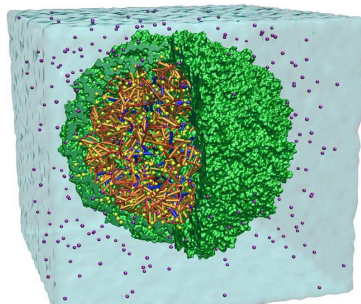
Fig. 1 Amino acids and peptides intercalated in hydrated LDH.

MD Simulations of a Complete Life Form: The Structure of a Satellite Tobacco Mosaic Virus



Freddolino et al. *Structure*, 14, 437–449 (2006)

- ◆ All-atom MD simulation of a complete virus, the satellite tobacco mosaic virus.
- ◆ $N \sim 1$ million atoms
- ◆ NAMD 2.5 MD program
- ◆ CHARMM22 force field for proteins; CHARMM27 for nucleic acids; TIP3P for water
- ◆ Total time ~ 50 ns / $\Delta t = 1$ fs
- ◆ Multiple time step algorithm:
 - ✓ bonded interactions - every time step
 - ✓ short-range nonbonded - every 2 time steps
 - ✓ long-range electrostatic - every 4 time steps
- ◆ Periodic boundary conditions, long-range electrostatics by particle-mesh Ewald
- ◆ 256 Altix nodes at NCSA / 1.1 ns per day



MD Simulations of a Satellite Tobacco Mosaic Virus

- ◆ Protein capsid (green) is enveloping the RNA
- ◆ The RNA backbone is highlighted red; the bases are drawn as cylinders; orange is used for double-stranded RNA regions; blue is used for single-stranded regions.
- ◆ The STMV particle is solvated in a $220 \times 220 \times 220 \text{ \AA}^3$ water box.
- ◆ Ions, added to neutralize negative charges of the RNA and positive charges of the coat proteins, are drawn in yellow (magnesium) and purple (chloride).

Freddolino et al. *Structure*, 14, 437–449 (2006)

Table 1. Simulated Systems

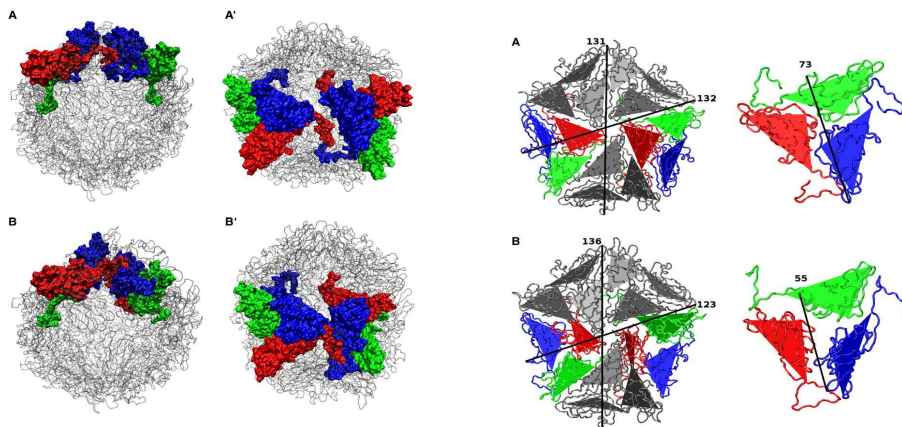
Name	Simulated System	Temperature (K)	Time (ns)	Atoms	System Size
simFULL	RNA/capsid assembly	298	13	1,066,628	$220 \text{ \AA} \times 220 \text{ \AA} \times 220 \text{ \AA}$
simCAPSID ₃₁₀	Capsid alone	310	10	932,500	$210 \text{ \AA} \times 210 \text{ \AA} \times 210 \text{ \AA}$
simCAPSID _{298A}	Capsid alone	298	10	932,500	$210 \text{ \AA} \times 210 \text{ \AA} \times 210 \text{ \AA}$
simCAPSID _{298B}	Capsid alone	298	10	1,068,969	$220 \text{ \AA} \times 220 \text{ \AA} \times 220 \text{ \AA}$
simRNA	RNA alone	298	10	388,000	$160 \text{ \AA} \times 166 \text{ \AA} \times 160 \text{ \AA}$

In the left column, conventional names of the simulations, as used throughout the paper, are defined. In the "Atoms" column, the full number of atoms simulated, including the atoms of protein and RNA, as well as of the surrounding solution (water and ions), is shown; in the case of simFULL, the simulated system was comprised of 899,565 water atoms, 135,960 protein atoms, 30,330 nucleic acid atoms, and 773 ions.

MD Simulations of a Satellite Tobacco Mosaic Virus

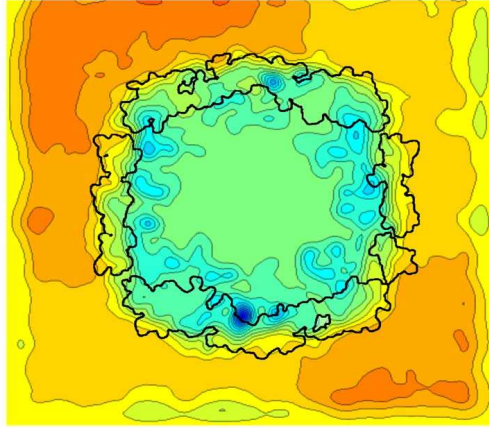
Freddolino et al. *Structure*, 14, 437–449 (2006)

Protein capsid collapse in the absence of RNA (after 10 ns)



MD Simulations of a Satellite Tobacco Mosaic Virus

Freddolino et al. *Structure*, 14, 437–449 (2006)



- ◆ Electrostatic potential distribution in a plane cut through the virion (averaged over 13 ns MD).
- ◆ The square cell shown in the picture is $220 \text{ \AA} \times 220 \text{ \AA}$.
- ◆ Contours of the capsid are highlighted by the thick black line.
- ◆ Mg^{2+} ions were initially placed in the vicinity of RNA, Cl^- ions were distributed in the surrounding water.
- ◆ The Cl^- ions moved almost freely during the simulation; $D_{\text{Cl}} = 1.5 \times 10^{-5} \text{ cm}^2/\text{s} \Rightarrow \sim \text{bulk}$
- ◆ Mg^{2+} ions remained attached to RNA, even exchange of Mg^{2+} places on RNA was rare.

Check for updates

OPEN ACCESS

EDITED BY
Adolfo Poma,
Polish Academy of Sciences, Poland

REVIEWED BY
Rosana Collepardo,
University of Cambridge, United Kingdom
Roberto Cowino,
Frankfurt Institute for Advanced Studies,
Germany

*CORRESPONDENCE
Siewert J. Marrink,
s.j.marrink@rug.nl

SPECIALTY SECTION
This article was submitted to Theoretical and Computational Chemistry, a section of the journal Frontiers in Chemistry

RECEIVED 23 November 2022
ACCEPTED 09 January 2023
PUBLISHED 18 January 2023

CITATION
Stevens JA, Grünewald F, van Tilburg PAM, König M, Gilbert BR, Brier TA, Thornburg ZR, Luthey-Schulten Z and Marrink SJ (2023) Molecular dynamics simulation of an entire cell.

Molecular dynamics simulation of an entire cell

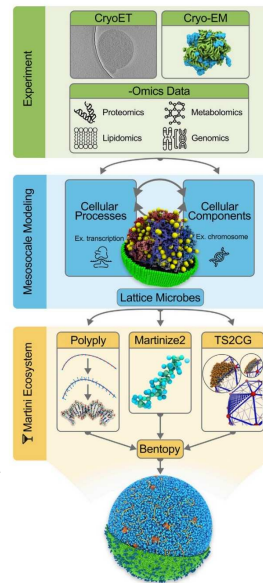
Jan A. Stevens¹, Fabian Grünewald¹, P. A. Marco van Tilburg¹, Melanie König¹, Benjamin R. Gilbert², Troy A. Brier², Zane R. Thornburg², Zaida Luthey-Schulten² and Siewert J. Marrink^{1*}

¹Molecular Dynamics Group, Groningen Biomolecular Sciences and Biotechnology Institute, University of Groningen, Groningen, Netherlands, ²Department of Chemistry, University of Illinois at Urbana-Champaign, Urbana, Champaign, IL, United States

The ultimate microscope, directed at a cell, would reveal the dynamics of all the cell's components with atomic resolution. In contrast to their real-world counterparts, computational microscopes are currently on the brink of meeting this challenge. In this perspective, we show how an integrative approach can be employed to model an entire cell, the minimal cell, JCVI-syn3A, at full complexity. This step opens the way to interrogate the cell's spatio-temporal evolution with molecular dynamics simulations, an approach that can be extended to other cell types in the near future.

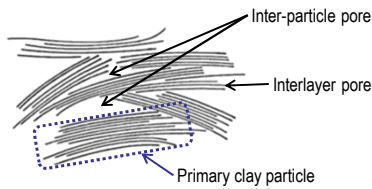
KEYWORDS

JCVI-syn3A, minimal cell, Martini force field, integrative modeling, coarse grain, polyply



Particle Edges: Quantum (Ab Initio) Molecular Dynamics to Address the Chemical Reactivity

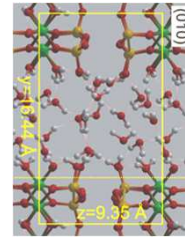
Aggregate of clay particles



- Use Q.M. to calculate energies at each time step (Schrödinger equation)
- Allows for chemical reaction
- Follow reactions through time
- Very expensive computationally
- $\sim n \times 100$ atoms; $\sim 15 \times 15 \times 15$ Å periodic box; $t \sim 10-50$ ps

H-bonding and proton exchange at the edges of clay particles

- H-exchange among surface sites occurs by a proton channel (wire) of H-bonds involving surface $-OH$ and H_2O
- Rate of exchange is controlled by the rate of H_2O rearrangement near the surface, not by individual H-exchange reactions

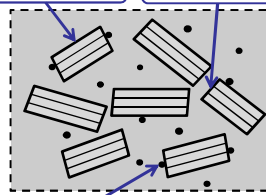


S.V.Churakov, *Geochim. Cosmochim. Acta*, **71**, 1130-1144 (2007)
 S.V.Churakov, *Amer. Mineral.*, **94**, 156-165 (2009)
 X. Liu et al., *Geochim. Cosmochim. Acta* (2012, 2013, 2014, 2015)
 S. Tazi et al., *Geochim. Cosmochim. Acta*, **94** 1-11 (2012)

ClayFF Parametrization for Clay Particle Edges

M.Pouvreau, PhD Thesis, Dec. 2016

Basal surface Edge surface

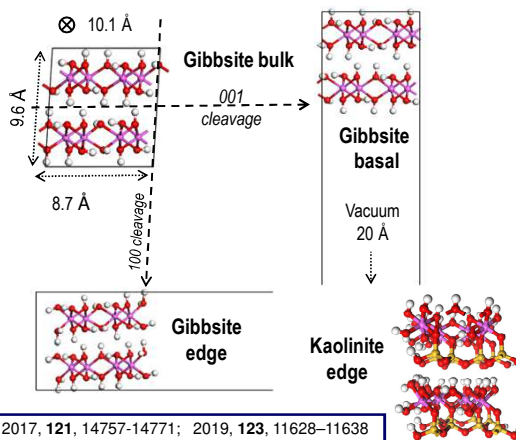


New special ClayFF M-O-H bending terms

$$U_{\text{ClayFF-MOH}} = U_{\text{ClayFF-orig}} + U_{\text{M-O-H}} = U_{\text{ClayFF-orig}} + k(\theta - \theta_0)^2$$

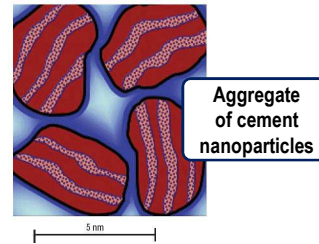
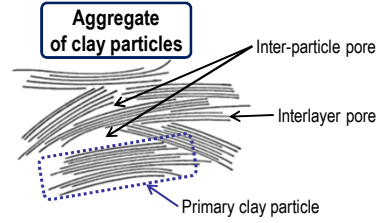
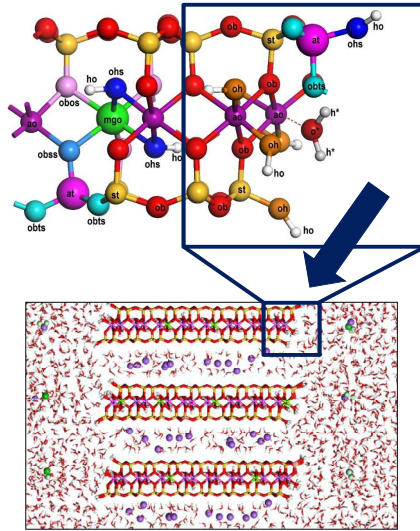
k and θ_0 have to minimize the differences between DFT and ClayFF-MOH results

- **Brucite, gibbsite, kaolinite** edges
- 3D periodic boundary conditions
- Cells size:
 - ✓ $N_{\text{atoms}} \sim 100$ for DFT+parametrization;
 - ✓ $N_{\text{atoms}} \sim 2500$ for classical MD



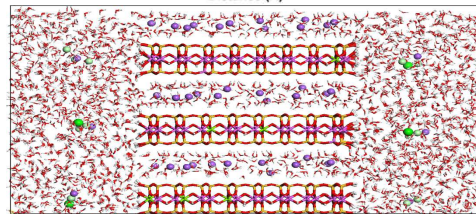
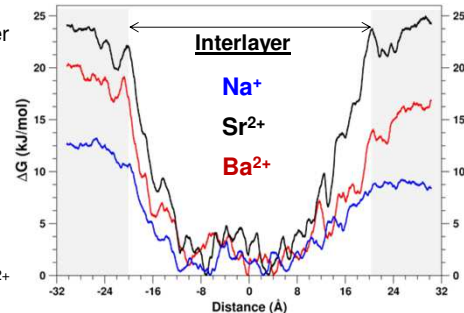
Pouvreau, Greathouse, Cygan, Kalinichev, *J.Phys.Chem.C*, 2017, **121**, 14757-14771; 2019, **123**, 11628-11638

Next: Adsorption at the Particle Edges and Mesoscale Modeling of Nanoparticle Aggregates



(010) Montmorillonite Edge: Interlayer vs Interface Adsorption of NORM Cations (H2020 ShaleX Project)

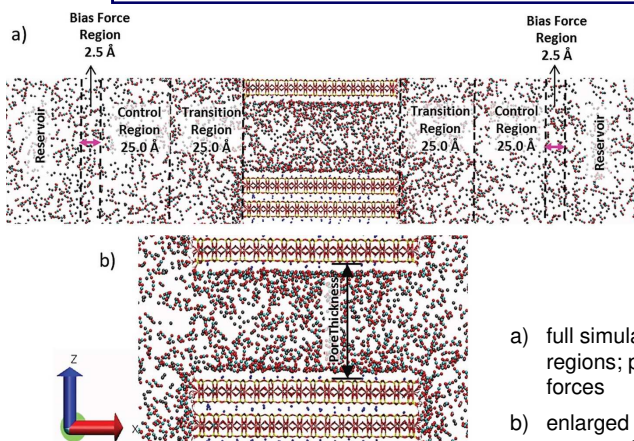
- ▶ All cations are more stable in the interlayer compared to the interfacial region
- ▶ The associated average free energy gain are as follows :
 - ~10 kJ/mol for Na⁺
 - ~25 kJ/mol for Sr²⁺
 - ~19 kJ/mol for Ba²⁺
- ▶ The energy gain when Na⁺ enters the interlayer region is almost doubled for Sr²⁺ and Ba²⁺: 1 Sr²⁺/Ba²⁺ for 2 Na⁺ ions.
- ▶ This is consistent with our statistical analyses showing that ~70% of Sr²⁺/Ba²⁺ initially present in the interfacial region migrate in the interlayers during the simulations
- ▶ There are noticeable energy barriers at the (010) edge for Sr²⁺/Ba²⁺ to enter the MMT interlayers



B.F.Ngouana et al., *J.Phys.Chem.C*, 2025, in prep.

CH₄/CO₂ Partitioning in Clay Nano- and Meso-Pores: Molecular Dynamics Modeling with Constant Reservoir Composition

N.Loganathan, G.M.Bowers, B.F.Ngouana-Wakou, A.G.Kalinichev, R.J.Kirkpatrick, O.Yazaydin
PCCP, 21, 6917-6924 (2019); *JPCC*, 124, 2490–2500 (2020)



Scheme of the simulation cells used in the constant reservoir composition molecular dynamics, CRC-MD calculations of CO₂/CH₄ partitioning into pores bounded by montmorillonite basal surfaces

- a) full simulation cell showing the different regions; pink arrows represent bias forces
- b) enlarged image of the silt-like pore and montmorillonite T-O-T layers

Energetics and Mechanism of Clay and Swelling (I)

THE JOURNAL OF
 PHYSICAL CHEMISTRY
 Letters

Cite This: *J. Phys. Chem. Lett.* 2019, 10, 3704–3709

Letter
 pubs.acs.org/JPCLE

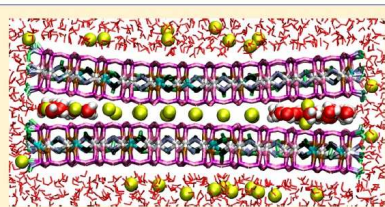
Revealing Transition States during the Hydration of Clay Minerals

Tuan A. Ho,^{*} Louise J. Criscenti,[†] and Jeffery A. Greathouse[‡]

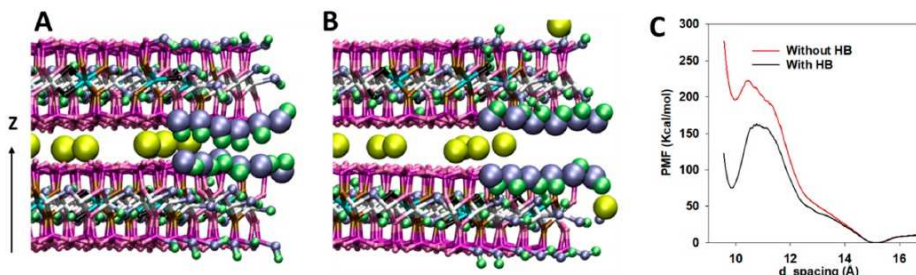
Geochemistry Department, Sandia National Laboratories, Albuquerque, New Mexico 87185, United States

[†] Supporting Information

ABSTRACT: A molecular-scale understanding of the transition between hydration states in clay minerals remains a challenging problem because of the very fast stepwise swelling process observed from X-ray diffraction (XRD) experiments. XRD profile modeling assumes the coexistence of multiple hydration states in a clay sample to fit the experimental XRD pattern obtained under humid conditions. While XRD profile modeling provides a macroscopic understanding of the heterogeneous hydration structure of clay minerals, a microscopic model of the transition between hydration states is still missing. Here, for the first time, we use molecular dynamics simulation to investigate the transition states between a dry interlayer, one-layer hydrate, and two-layer hydrate. We find that the hydrogen bonds that form across the interlayer at the clay particle edge make an important contribution to the energy barrier to interlayer hydration, especially for initial hydration.



Energetics and Mechanism of Clay and Swelling (II)



- ▶ Edge H-bonds between TOT layers in the dry state act like a gate, preventing the passage of water molecules and ions into the interlayer
- ▶ Swelling process begins by breaking those H-bonds so that H₂O molecules can diffuse into the interlayer
- ▶ It is possible that proton transfer could significantly affect the mechanism and energy differences between hydration states

Ho et al., *J.Phys.Chem.Lett.*, **10**, 3704-3709 (2019)

LANGMUIR

Cite This: *Langmuir* XXXX, XXX, XXX–XXX

Article

pubs.acs.org/Langmuir

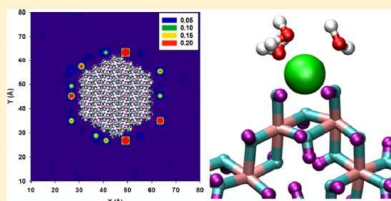
Enhanced Ion Adsorption on Mineral Nanoparticles

Tuan A. Ho,*¹ Jeffery A. Greathouse,*² Andrew S. Lee, and Louise J. Criscenti*²

Geochemistry Department, Sandia National Laboratories, Albuquerque, New Mexico 87185, United States

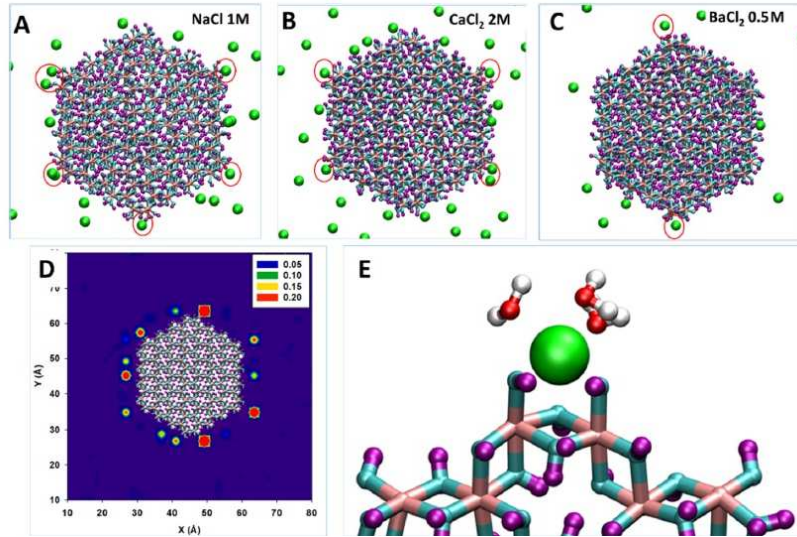
¹ Supporting Information

ABSTRACT: Classical molecular dynamics simulation was used to study the adsorption of Na⁺, Ca²⁺, Ba²⁺, and Cl⁻ ions on gibbsite edge (1 0 0), basal (0 0 1), and nanoparticle (NP) surfaces. The gibbsite NP consists of both basal and edge surfaces. Simulation results indicate that Na⁺ and Cl⁻ ions adsorb on both (1 0 0) and (0 0 1) surfaces as inner-sphere species (i.e., no water molecules between an ion and the surface). Outer-sphere Cl⁻ ions (i.e., one water molecule between an ion and the surface) were also found on these surfaces. On the (1 0 0) edge, Ca²⁺ ions adsorb as inner-sphere and outer-sphere complexes, whereas on the (0 0 1) surface, outer-sphere Ca²⁺ ions are the dominant species. Ba²⁺ ions were found as inner-sphere and outer-sphere complexes on both surfaces. Calculated ion surface coverages indicate that, for all ions, surface coverages are always higher on the basal surface compared to those on the edge surface. More importantly, surface coverages for cations on the gibbsite NP are always higher than those calculated for the (1 0 0) and (0 0 1) surfaces. This enhanced ion adsorption behavior for the NP is due to the significant number of inner-sphere cations found at NP corners. Outer-sphere cations do not contribute to the enhanced surface coverage. In addition, there is no ion adsorption enhancement observed for the Cl⁻ ion. Our work provides a molecular-scale understanding of the relative significance of ion adsorption onto gibbsite basal versus edge surfaces and demonstrates the corner effect on ion adsorption on NPs.

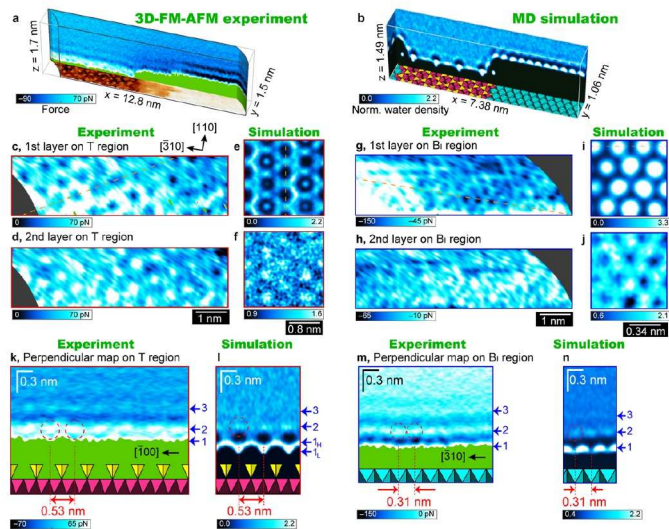


Enhanced Ion Adsorption on Nanoparticle Edges and Corners

Ho et al., *Langmuir*, 34, 5926-5934 (2018)

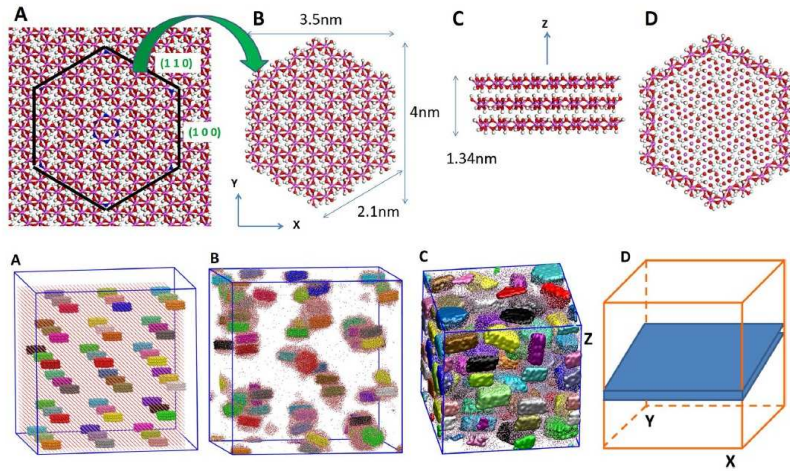


AFM vs MD of Chlorite Step Edges



Yamada et al., *Nature Comm.*, (2017)

Atomistic Mechanisms of Clay Nano-Particles Aggregation, Compaction, and Dewatering

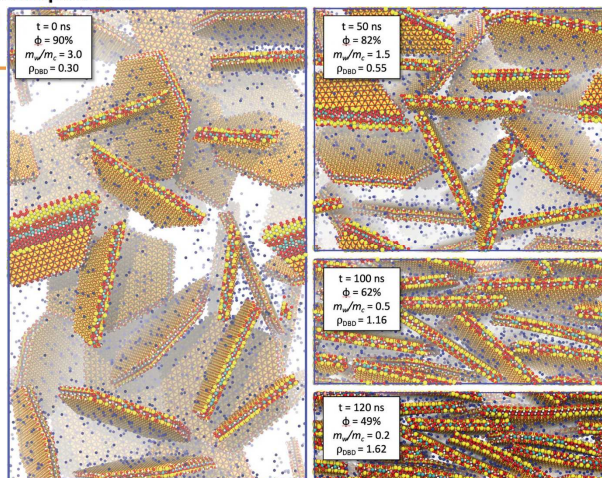


Ho et al., *Scientific Reports*, 7, 15286 (2017)

Large-Scale Molecular Dynamics Simulation of the Dehydration of a Suspension of Smectite Clay Nanoparticles

Thomas R. Underwood* and Ian C. Bourg*

Cite This: *J. Phys. Chem. C* 2020, 124, 3702–3714



Coordination Chemistry Reviews 526 (2025) 216347

Contents lists available at ScienceDirect

Coordination Chemistry Reviews

journal homepage: www.elsevier.com/locate/ccr

Molecular modeling of clay minerals: A thirty-year journey and future perspectives

Annan Zhou^{a,*}, Jiawei Du^a, Ali Zaoui^b, Wassila Sekkal^b, Muhammad Sahimi^c

^a Discipline of Civil and Infrastructure Engineering, School of Engineering, Royal Melbourne Institute of Technology (RMIT), Victoria 3001, Australia
^b Univ. Lille, IMT Nord Europe, JUNIA, Univ. Artois, ULR 4515 - LGCgE, Laboratoire de Génie Civil et Geo-Environnement, F-59000 Lille, France
^c Mark Family Departments of Chemical Engineering and Materials Science, University of Southern California, Los Angeles, CA 90089-1211, USA

ARTICLE INFO

Keywords:
 Clay minerals
 Molecular simulation
 Nanoscale energies
 Mechanical properties
 Diffusion
 Adsorption

ABSTRACT
 The growing demand for a deeper understanding and improved utilization need for a comprehensive review of the latest advancements and future modeling. This paper addresses this need by providing an in-depth review of the past 30 years. Beginning with an introduction to classification of clay minerals and a concise historical overview, this paper delves into the mechanical properties of clay minerals, with detailed discussions on force fields, computational pack nanoscale energy variation within clay minerals is described, covering by ion energies. The analysis is then extended to the nanoscale mechanical

Drug delivery

Water purification

Energy storage

Catalysis

NE-M1-PRI12ENP – Integrated Nuclear Engineering Project, February-June 2025
 “Molecular modeling of materials for nuclear waste disposal applications”

Challenges of the Quantitative Analysis of Interfacial Structure at the Irregular Surfaces

H₂O on hematite, Spagnoli et al., (2009)

a

b

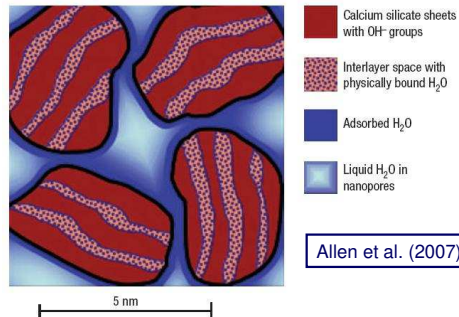
➤ “Real surfaces” should probably look more like this

➤ Some order is evident, but is much harder to quantify than in the case of flat surfaces

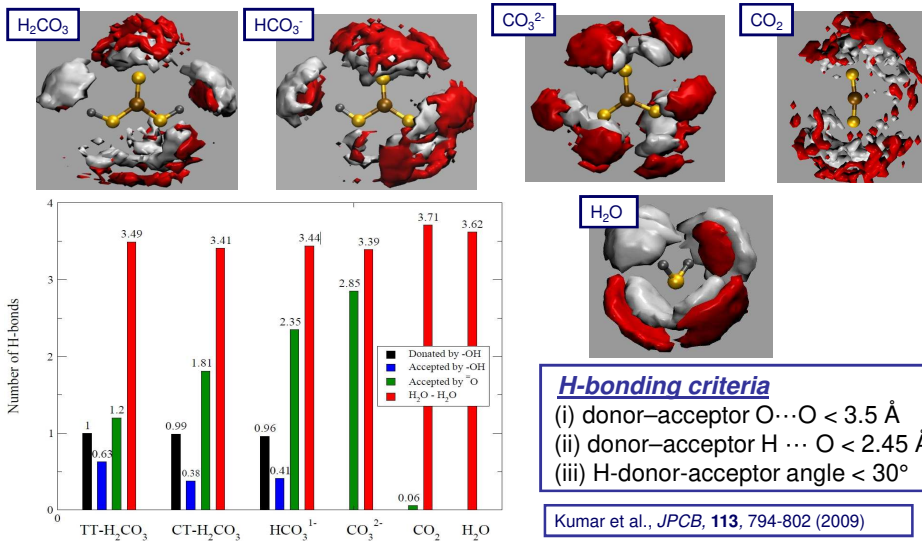
NE-M1-PRI12ENP – Integrated Nuclear Engineering Project, February-June 2025
 “Molecular modeling of materials for nuclear waste disposal applications”

Challenges of the Quantitative Analysis of Interfacial Structure at the Irregular Surfaces

- Simple 1-D and 2-D approaches do not work
- Even though we have full atomistic description of a large system, there are no obvious ways to extract useful information
- Need to develop new approaches to analyze adsorption, conformations, H-bonding, diffusion, beyond 1-D and 2-D simplifications
- Structure and dynamics in topologically complex nanoporous space, e.g., between aggregated nanoparticles

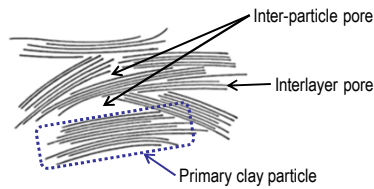


H-Bonding Structure Around Aqueous Carbonic Species



Particle Edges: Quantum (Ab Initio) Molecular Dynamics to Address **Chemical Reactivity**

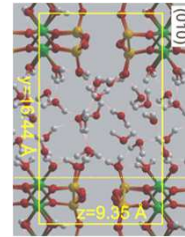
Aggregate of clay particles



- Use Q.M. to calculate energies at each time step (Schrödinger equation)
- Allows for chemical reaction
- Follow reactions through time
- Very expensive computationally
- $\sim n \times 100$ atoms; $\sim 15 \times 15 \times 15$ Å periodic box; $t \sim 10-50$ ps

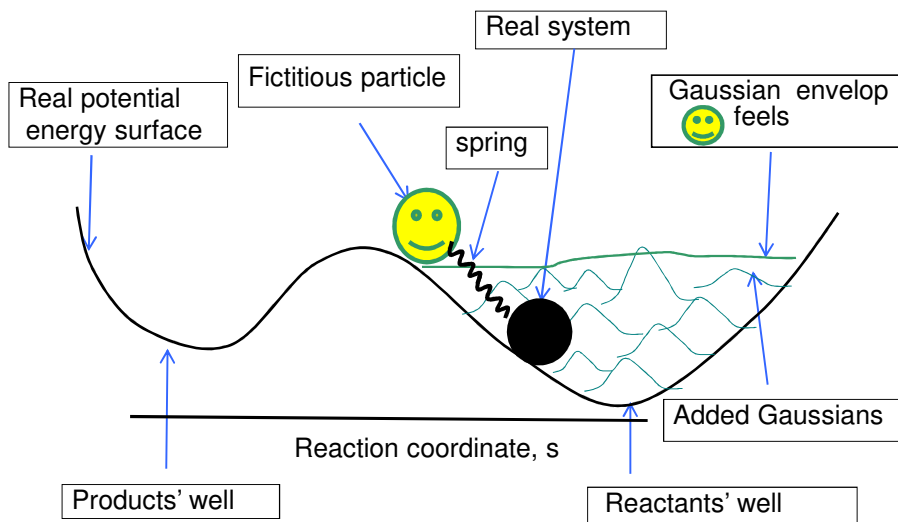
H-bonding and proton exchange at the edges of clay particles

- H-exchange among surface sites occurs by a proton channel (wire) of H-bonds involving surface $-OH$ and H_2O
- Rate of exchange is controlled by the rate of H_2O rearrangement near the surface, not by individual H-exchange reactions



S.V.Churakov, *Geochim. Cosmochim. Acta*, **71**, 1130-1144 (2007)
 S.V.Churakov, *Amer. Mineral.*, **94**, 156-165 (2009)
 X. Liu et al., *Geochim. Cosmochim. Acta* (2012, 2013, 2014, 2015)
 S. Tazi et al., *Geochim. Cosmochim. Acta*, **94** 1-11 (2012)

Classical or Ab Initio Metadynamics – A Possible Solution



Ab-initio Metadynamics

“Biased dynamics” through an extended Lagrangian formulation.

Laio & Parrinello, *PNAS*, **99**, 12562 (2002)

$$\mathcal{L}_{\text{MTD}} = \mathcal{L}_{\text{CP}} + \frac{1}{2}\mu\dot{s}^2 - \frac{1}{2}k(S(R) - s)^2 - V(t, s)$$

\mathcal{L}_{CP} - the standard CP Lagrangian

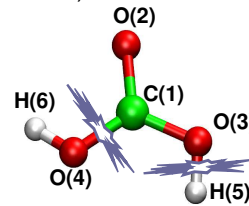
$S(R)$ - the “collective variable”

s - the position of the fictitious particle (reaction coordinate),

μ - its mass

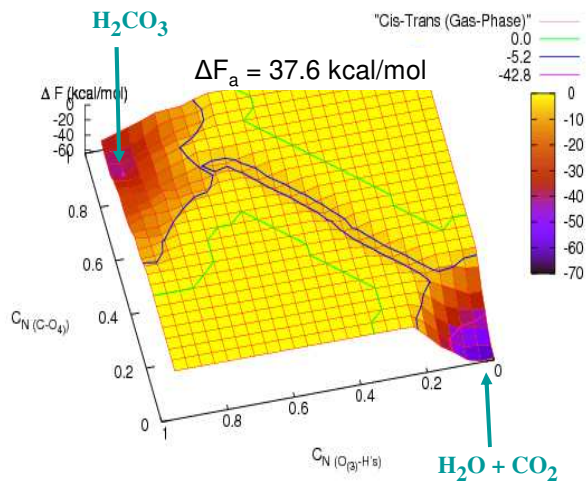
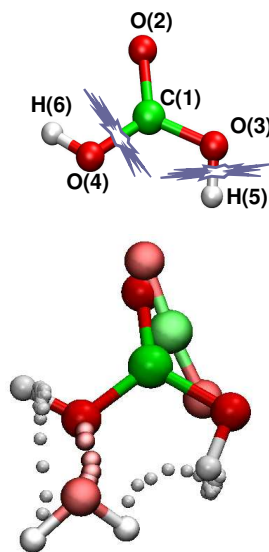
$$V(t, s) = W \sum_{t_i < t} \exp\left\{-\frac{(s - s(t_i))^2}{2\sigma^2}\right\}$$

W - width & σ - height of the Gaussians



NE-M1-PRI12ENP – Integrated Nuclear Engineering Project, February-June 2025
“Molecular modeling of materials for nuclear waste disposal applications”

Free Energy Surfaces for Dissociation of the Cis-Trans(2) - H_2CO_3 in the Gas-Phase

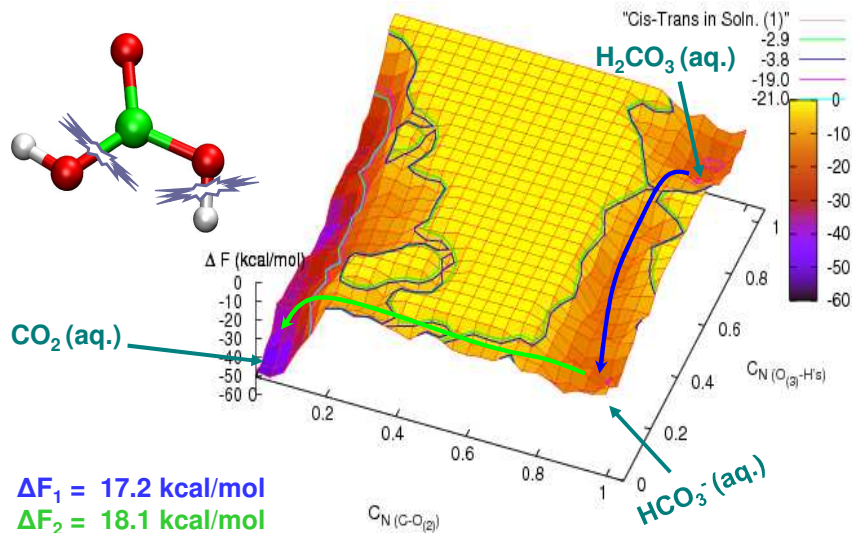


Kumar, Kalinichev & Kirkpatrick, *J.Chem.Phys.*, **126**, 204315 (2007)



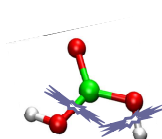
NE-M1-PRI12ENP – Integrated Nuclear Engineering Project, February-June 2025
“Molecular modeling of materials for nuclear waste disposal applications”

Free Energy Surface of Cis-Trans(2) - H₂CO₃ Dissociation in Aqueous Solution

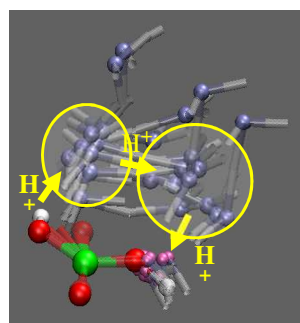
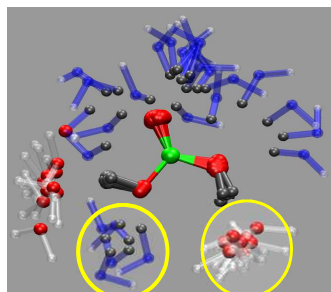


NE-M1-PRI12ENP – Integrated Nuclear Engineering Project, February-June 2025
 “Molecular modeling of materials for nuclear waste disposal applications”

Mechanism of Cis-Trans - H₂CO₃ Dissociation in Aqueous Solution



- A proton channel (“proton wire”) along the H-bonding network facilitates the dissociation
- The “proton wire” could be as short as just 3 H-transfer events!
- **Metadynamics calculation is hard to control if more than 2 collective variable are used, which is inevitable for multiple H-transfer events in aqueous environment**



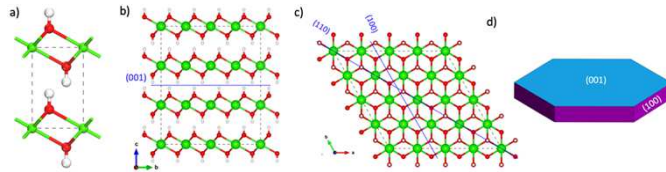
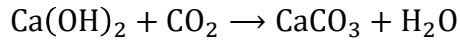
Superimposed snapshots of H₂O distribution from equilibrium MD

Kumar, Kalinichev & Kirkpatrick, *JPCB*, **113**, 794-802 (2009)

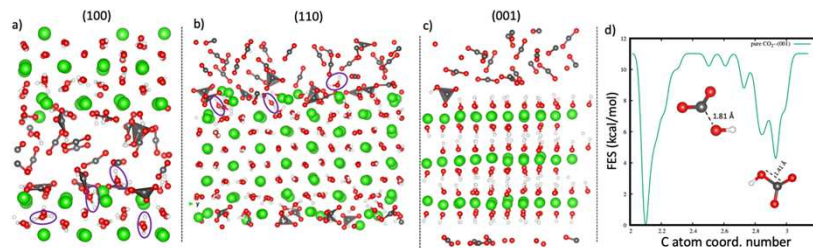


NE-M1-PRI12ENP – Integrated Nuclear Engineering Project, February-June 2025
 “Molecular modeling of materials for nuclear waste disposal applications”

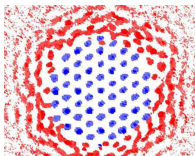
Reactivity of Supercritical CO₂ with Portlandite Surfaces (AIMD + Metadynamics)



S.Mutisya, A.G.Kalinichev, *Minerals*, **11**, 509 (2021)



Next Generation Force Field is Necessary for Large Scale MD Simulations



Spagnoli et al., (2009)



Ohlin et al., (2009)

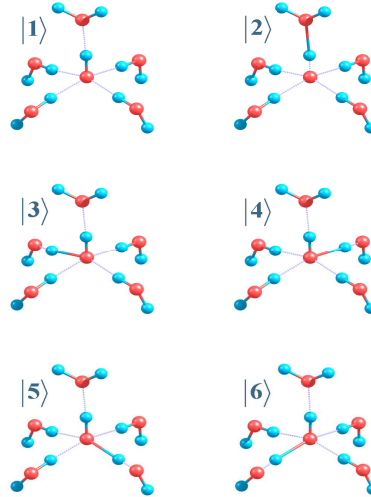
- How the structure and dynamics at the interface will change, if the surface is reactive, e.g., through H-transfer?
- What happens when the surface reactivity is very different at different sites?
- Quantum chemical treatment can be accurate, but it is computationally very expensive for complex systems, even with the next generation of high performance computers
- There are several approaches (e.g., ReaxFF), but no good solution yet
- Another possible compromise solution may be multi-state empirical valence bond (MS-EVB) parameterization (e.g., G.A.Voth, *Acc.Chem.Res.* **39**, 143-150, 2006)

Empirical Valence Bond (EVB) Approach to the Molecular Modeling of Reactive Aqueous Solutions

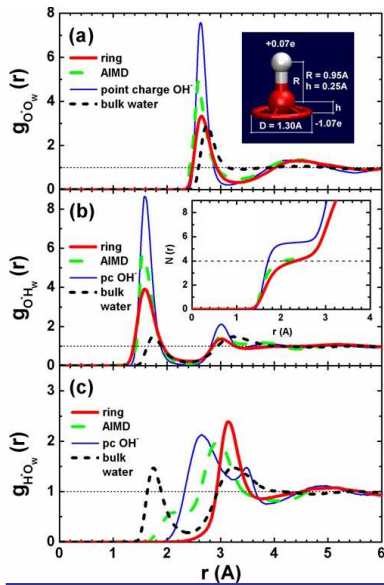
- The symmetrical EVB $N \times N$ matrix consists of N diagonal elements (diabatic states) and $N(N-1)/2$ off-diagonal "coupling terms"
- The matrix diagonalization yields the ground state potential energy surface and forces applied to each atom of the system

$$\mathbf{H}(\mathbf{x}) = \begin{pmatrix} h_{11}(\mathbf{x}) & h_{12}(\mathbf{x}) & h_{13}(\mathbf{x}) & h_{14}(\mathbf{x}) \\ h_{21}(\mathbf{x}) & h_{22}(\mathbf{x}) & 0 & 0 \\ h_{31}(\mathbf{x}) & 0 & h_{33}(\mathbf{x}) & 0 \\ h_{41}(\mathbf{x}) & 0 & 0 & h_{44}(\mathbf{x}) \end{pmatrix}$$

$$U(\mathbf{x}) = \sum_{i,j} c_i^{(0)} c_j^{(0)} h_{ij}(\mathbf{x}) \quad \mathbf{F}(\mathbf{x}) = - \sum_{i,j} c_i^{(0)} c_j^{(0)} \frac{\partial h_{ij}(\mathbf{x})}{\partial \mathbf{x}}$$

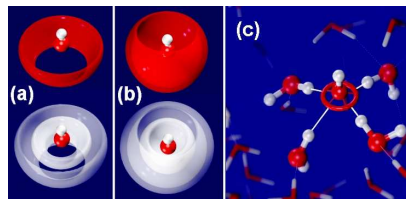


Charged Ring Model of OH⁻ in Aqueous Solution



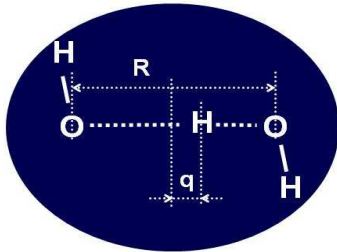
Ufimtsev et al., *Chem. Phys. Lett.*, **442**, 128-133 (2007)

- ◆ A hard massless ring is attached to the oxygen atom, and carries the atom's negative charge
- ◆ As a result, water molecules mostly interact with the ring rather than with the oxygen atom
- ◆ Hydroxyl orientation is stabilized by the ring
- ◆ The negative charge is "spread", thus effectively decreasing the ion's coordination number
- ◆ The ring is shifted down from the oxygen atom to favor tetrahedral configuration of the 1st solvation shell



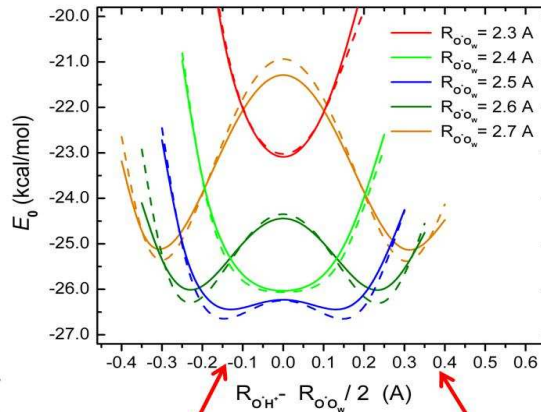
- ◆ Spatial distribution functions of the oxygen (red) and hydrogen (white) atoms of the OH⁻ first hydration shell H₂O molecules, (a) charged-ring, (b) point-charge OH⁻ ion models.

Ab Initio vs. EVB: Potential Energy



• The EVB potential parameters are fitted to reproduce the *ab initio* potential energy surface for the reaction H-O-H...O-H in water

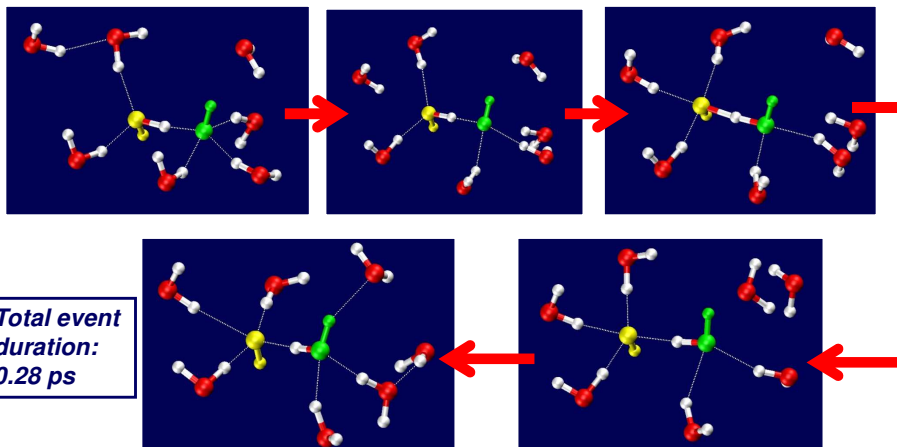
Ufimtsev, Kalinichev, Martinez, Kirkpatrick, *PCCP*, **11**, 9420-9430 (2009)



MP2/aug-cc-pVDZ
COSMO (dashed lines)

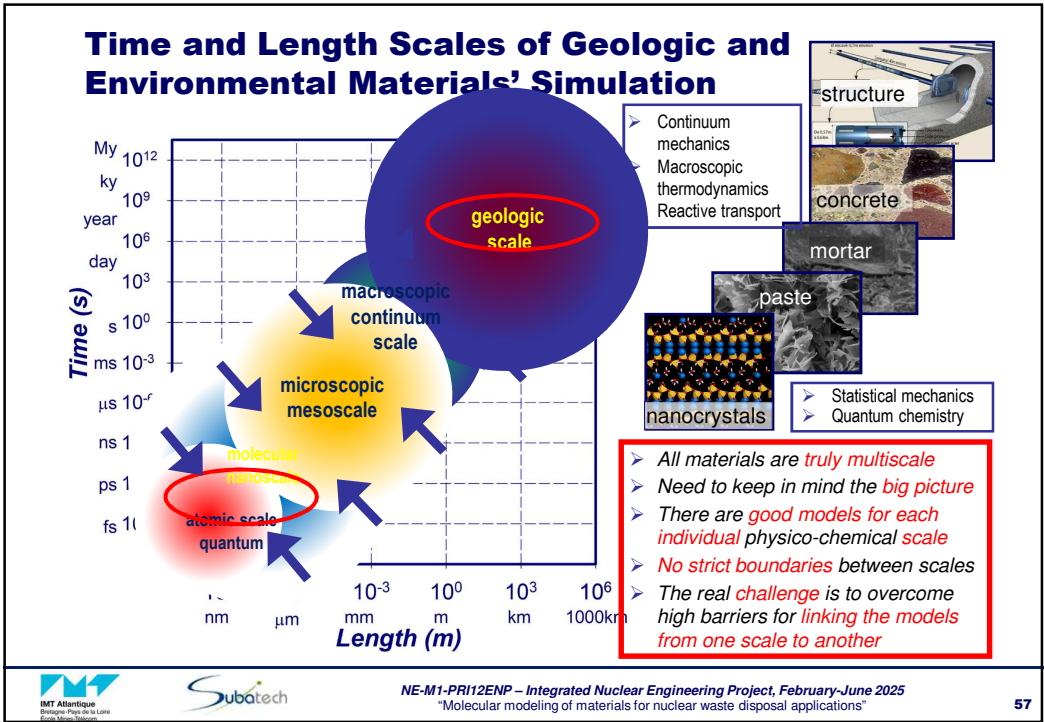
MS-EVB model
(solid lines)

An Example of a HO...H...OH Proton Hopping Event



- **Under-coordinated** 3-bonded environment of OH⁻(aq) is an important step facilitating the reaction
- Rearrangements of H-bonds in the **second hydration shell** are important in order to successfully complete the process

Ufimtsev, Kalinichev, Martinez, Kirkpatrick, *PCCP*, **11**, 9420-9430 (2009)

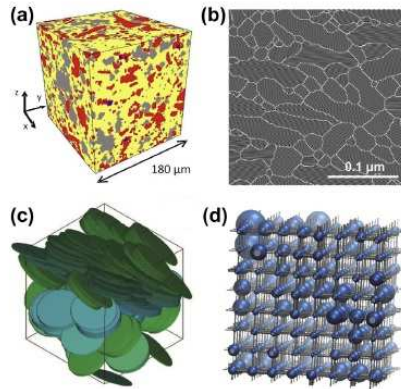


Multiscale Problems & Approaches (I)

Weinberger, C. R.; Tucker, G. J.(Eds.)
Multiscale Materials Modeling for Nanomechanics. Springer International Publishing, 2016, 554pp.

NE-M1-PRI12ENP – Integrated Nuclear Engineering Project, February-June 2025
"Molecular modeling of materials for nuclear waste disposal applications"
58

Multiscale Problems & Approaches (II)



Marry, V.; Rotenberg, B., Upscaling Strategies for Modeling Clay-Rock Properties. In *Developments in Clay Science*, Tournassat, C.; Steefel, C. I.; Bourg, I. C.; Bergaya, F., Eds. Elsevier: 2015; Vol. 6, pp 399-417.

FIGURE 11.3 Models of representative elementary volume. (a) 3D mineralogical map of Calovo-Oxfordian clay obtained from X-ray tomography experiments. (Reprinted from Robinet et al. (2012), Copyright 2012, with permission of John Wiley & Sons, Inc.) (b) 2D grain structure used to model diffusion in montmorillonite. (Reprinted from Churakov et al. (2014), with permission from Elsevier.) (c) 3D packing of ellipsoids obtained using a potential of mean force from Molecular simulations. (Reprinted from Ebrahimi et al. (2014), Copyright 2014, AIP Publishing LLC.) (d) Pore network model (Copyright Amael Obliger).

Multiscale Problems & Approaches (III)

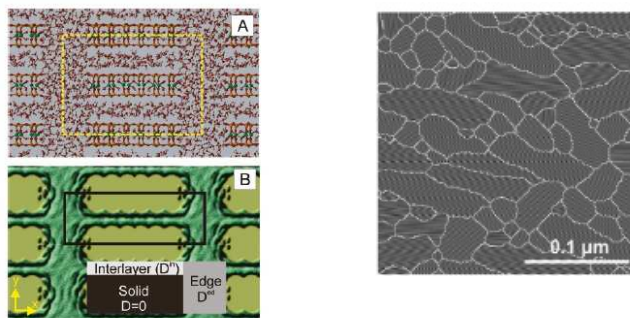


Figure 1. (A) Snapshot from MD simulations of pyrophyllite particles separated by two water layers. Oxygen, hydrogen, silica, and aluminum atoms are shown as red, gray, yellow, and green spheres, respectively. The simulation supercell is shown by the yellow dashed line. (B) A surface plot of the 2D probability density profile of water molecules from molecular dynamics simulations. Peak areas correspond to long residence times. In the overlay, light gray and gray areas indicate interlayer space and interparticle porosity, respectively, as assigned for the RW simulations. The diffusion coefficients D^m and D^p for these pore spaces were obtained from short (200 ps) MD trajectories resident in the corresponding domains. The solid phase domain impenetrable for water is shown as a black area. The simulation cell for the RW simulations is shown by the solid black line.

Churakov, S. V.; Gimmi, T., Up-Scaling of Molecular Diffusion Coefficients in Clays: A Two-Step Approach. *Journal of Physical Chemistry C* 2011, 115, 6703-6714

Multiscale Problems & Approaches (IV)

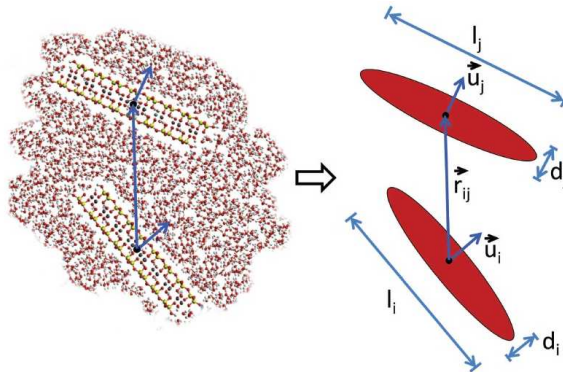


Figure 2. Interactions between two clay platelets are approximated by single-site potential functions for an ellipsoidal body (GB potential).

Ebrahimi, D.; Whittle, A. J.; Pellenq, R. J. M., Effect of polydispersity of clay platelets on the aggregation and mechanical properties of clay at the mesoscale. *Clays and Clay Minerals* **2016**, *64*, 425-437

Multiscale Problems & Approaches (V)

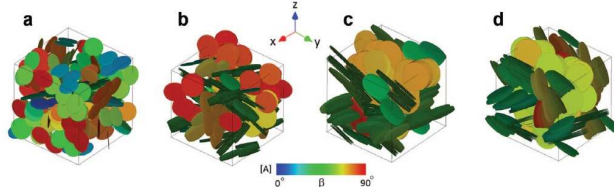


Figure 5. Examples of the final configuration of the system of particles with diameter $D=601$ Å at pressure $P=(a)$ 1 atm; (b) 10 atm; (c) 300 atm; and (d) 800 atm. The orientations of the particles are color coded according to the β angle, the orientation of their normal vector with respect to the Z axis (colorbar A). By increasing the pressure the spectrum of colors decreased as the stack size increased and the system became more ordered. At high pressure ($P=800$ atm), platelets started to slide against each other.

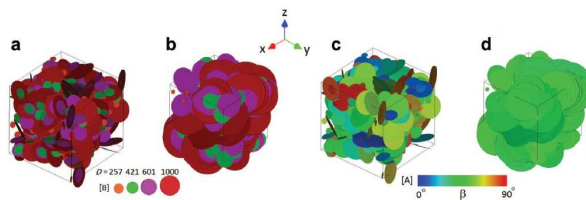
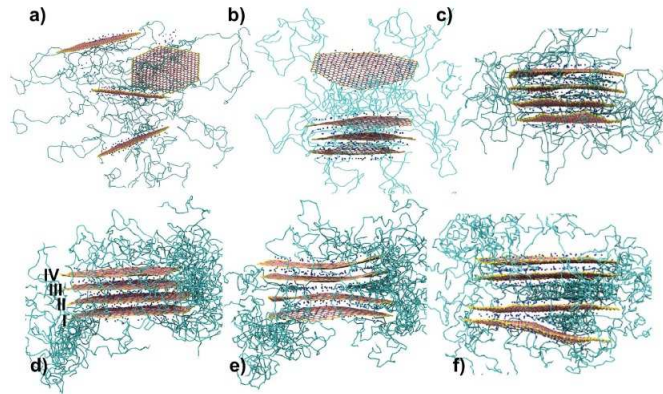


Figure 7. Examples of the final configuration of the polydisperse system of particles with diameters $D=257, 421, 601,$ and 1000 Å at pressure $P,(a,c)=1$ atm, (b, d) = 800 atm. In parts a and b, particles are color coded based on their size (colorbar B) and in parts c and d they are color coded according to the β angle, the orientation of their normal vector with respect to the Z axis (colorbar A). By increasing the pressure, the spectrum of color decreases as the system becomes more ordered (see c and d).

Ebrahimi et al., Effect of polydispersity of clay platelets on the aggregation and mechanical properties of clay at the mesoscale. *Clays and Clay Minerals* **2016**, *64*, 425-437

Multiscale Problems & Approaches (VI)



Suter, J. L.; Groen, D.; Coveney, P. V., Chemically specific multiscale modeling of clay-polymer nanocomposites reveals intercalation dynamics, tactoid self-assembly and emergent materials properties. *Advanced Materials* **2015**, *27*, 966-984

Multiscale Problems & Approaches (VII)

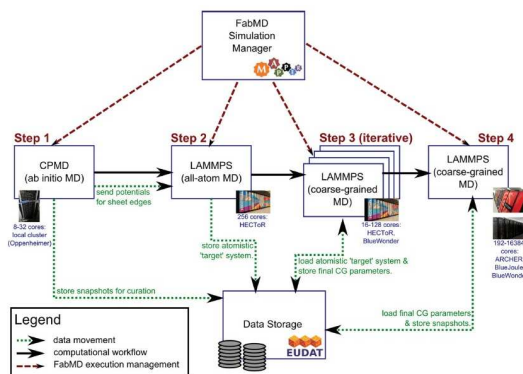


Figure 4. Overview of the computational and data workflow applied in our multiscale modeling scheme. We use the FabMD toolkit to help automate the four primary steps in our approach. These include ab initio calculations of the forces on the sheet edges (step 1, run on a departmental cluster), all-atom MD simulations to extract key distribution functions (step 2, run on a supercomputer), hundreds of small coarse-grained MD simulations performed iteratively to find the optimal parameters for the coarse-grained system (step 3, mostly run on a supercomputer), and finally the coarse-grained MD production runs (step 4, with simulations run on several different supercomputers). For each step in the workflow, we provide basic information about the HPC resources used below the description box. We use a distributed data-storage system, provided by EUDAT (<http://www.eudat.eu>), to facilitate the exchange of data between the different steps of the workflow and to curate the output of our simulations.

Suter, J. L.; Groen, D.; Coveney, P. V., Chemically specific multiscale modeling of clay-polymer nanocomposites reveals intercalation dynamics, tactoid self-assembly and emergent materials properties. *Advanced Materials* **2015**, *27*, 966-984

Nanoscale Prediction of the Thermal, Mechanical, and Transport Properties of Hydrated Clay on 10^6 - and 10^{15} -Fold Larger Length and Time Scales

Xiaojin Zheng* and Ian C. Bourg*

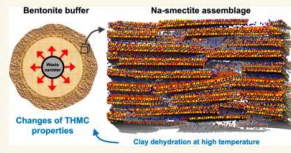
Cite This: <https://doi.org/10.1021/acsnano.3c05751>

Read Online

ACCESS | Metrics & More | Article Recommendations | Supporting Information

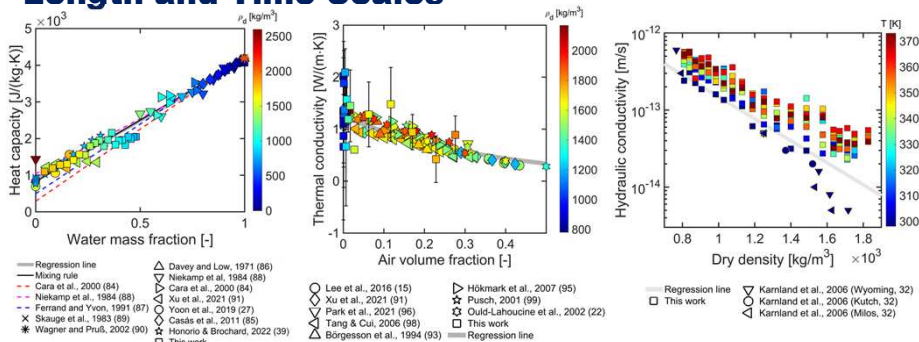
ABSTRACT: Coupled thermal, hydraulic, mechanical, and chemical (THMC) processes, such as desiccation-driven cracking or chemically driven fluid flow, significantly impact the performance of composite materials formed by fluid-mediated nanoparticle assembly, including energy storage materials, ordinary Portland cement, bioinorganic nanocomposites, liquid crystals, and engineered clay barriers used in the isolation of hazardous wastes. These couplings are particularly important in the isolation of high-level radioactive waste (HLRW), where heat generated by radioactive decay can drive the temperature up to at least 373 K in the engineered barrier. Here, we use large-scale all-atom molecular dynamics simulations of hydrated smectite clay nanoparticle assemblages to predict the fundamental THMC properties of hydrated compacted clay over a wide range of temperatures (up to 373 K) and dry densities relevant to HLRW management. Equilibrium simulations of clay-water mixtures at different hydration levels are analyzed to quantify material properties, including thermal conductivity, heat capacity, thermal expansion, suction, water and ion self-diffusivity, and hydraulic conductivity. Predictions are validated against experimental results for the properties of compacted bentonite clay. Our results demonstrate the feasibility of using atomistic-level simulations of assemblages of clay nanoparticles on scales of tens of nanometers and nanoseconds to infer the properties of compacted bentonite on scales of centimeters and days, a direct upscaling over 6 orders of magnitude in space and 15 orders of magnitude in time.

KEYWORDS: molecular dynamics simulation, radioactive waste isolation, bentonite barrier, THMC properties, clay dehydration, nanopore water



Zheng, Bourg (2023)
ACS Nano, 17, 19211-19223

From Nanoscale MD Simulations to the Prediction of Thermal, Mechanical, and Hydraulic Properties of Hydrated Clay on 10^6 - and 10^{15} -fold Larger Length and Time Scales



- Large-scale simulators rely critically on constitutive relations representing the THMC material properties of bentonite to predict the performance of bentonite buffers
- Empirical relations of previous studies were generally derived to fit individual experimental datasets
- Here, the insights gained from MD simulations and compilation of previous experimental results help to constrain the form of these empirical constitutive relations

Zheng, Bourg, ACS Nano, 17, 19211-19223 (2023)

Nonadditivity & Collective Motions (I)

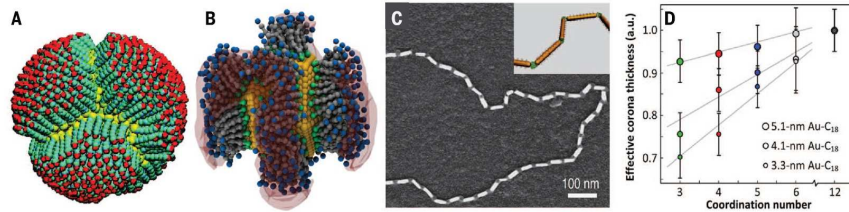


Fig. 3. Collective behavior of stabilizer molecules. (A and B) Snapshot of MD simulation of (A) spherical (65) and (B) icosahedral NPs (109) with charged groups at the core surface. For (B), isodensity surface of counterions and anions in the vicinity of the surface ligands is shown in pink. (C) Scanning electron microscopy image and schematic (inset) of the chains of end-modified gold nanorods (120). Scale bar, 100 nm. (D) Dependence of the effective thickness of the soft surface layer on the number of nearest neighbors in closely packed Au NPs (112). a.u., arbitrary units.

Silvera Batista, C. A.; Larson, R. G.; Kotov, N. A., Nonadditivity of nanoparticle interactions. *Science* **2015**, *350*, (6257)

Nonadditivity & Collective Motions (II)

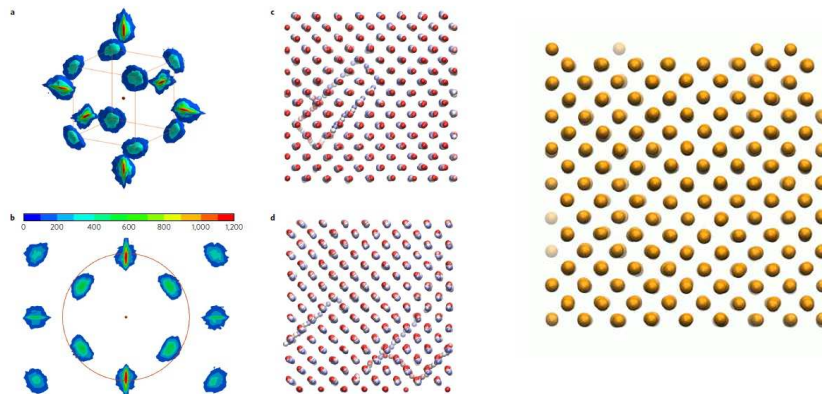


Figure 4 | Structure of bcc iron at 7,000 K and 360 GPa. a, Three-dimensional distribution of the probability density of atoms as a function of distance from the central atom. b, Projection of a on (110). The density in a and that in b are averaged over the atoms and the last 8,000 timesteps of the run of 18,000 timesteps duration. About half of the second neighbours density contributes to the coordination number, that is, the total coordination number is $8 + 6/2 = 11$. c, d, X (c) and Z (d) projections of five snapshots. The atoms in c and d are coloured according to the red-white-blue sequence corresponding to time progression. The snapshots are separated by 200 timesteps. The positions of the atoms are averaged using the 1,000 timesteps running window to average out the high-frequency vibrations. Note the diffusion confined to (110).

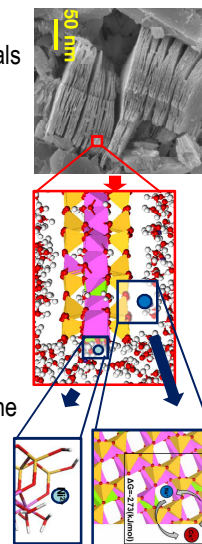
Belonoshko, A. B.; Lukinov, T.; Fu, J.; Zhao, J.; Davis, S.; Simak, S. I., Stabilization of body-centred cubic iron under inner-core conditions. *Nature Geoscience* **2017**, *10*, 312-317

Problems & Priorities

- **Quantitative analysis** of the structure and dynamics of **irregularly shaped interfaces**
- **Slow processes & rare events** (on the MD scale)
- **Chemical reactivity** on the relatively large time- and length- scales (**reactive FF**, QM-MM)
- **Upscaling MD to meso- and macro- scale** (multi-scale approaches, coarse-graining, etc.)
- **Collective / cooperative effects**

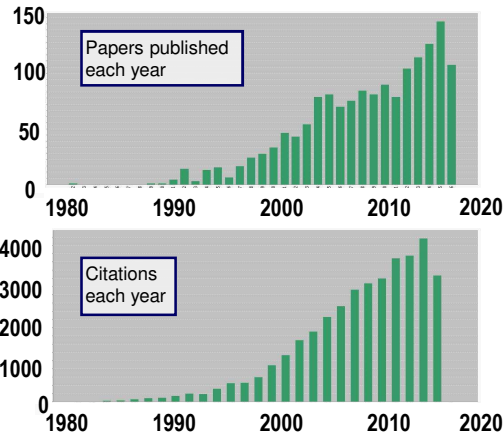
Conclusions and Outlook (I)

- Molecular computer modeling is a powerful tool to study many nano-scale phenomena in clay and cement chemistry, geochemistry, materials science, and environmental chemistry, complementary to other experimental physical and chemical methods already widely used to characterize properties of materials and their aqueous interfaces
- Molecular simulations are able to qualitatively, and often quantitatively, reproduce and predict the structure and properties clay and cement phases and their interfaces with aqueous solutions
- The ability to improve our physical understanding of the complex physical and chemical behavior of these systems and to unravel many fundamental atomic- and molecular-scale correlations between their structural, transport, spectroscopic, and thermodynamic properties is the most important and valuable feature of these techniques
- Being neither pure theory, nor pure experiment, such "computer experiments" can greatly stimulate the development of both theoretical and experimental studies of clay/water interfaces in the near future



Conclusions and Outlook (II)

- Good consistency of MD-simulated results with X-ray, NMR, INS, QENS measurements
- Simulations with larger **more realistic and diverse models** of reactive mineral-water interfaces are necessary
- New quantitative **multi-scale** approaches need to be developed
- Close **collaboration between experimental and molecular modeling** approaches is necessary
- New more powerful **peta- and exa-scale supercomputing** facilities are becoming extremely helpful in allowing to address the observed phenomena at much larger geochemically and environmentally relevant time- and length- scales
- **Bright future ahead!**



Questions for the final paper / report on one of the ~26 topics, e.g., 1 – clays; 2 – cement; 3 – TiO₂ surfaces; 4 – corrosion; 5 – organics, etc. <https://moodle.imt-atlantique.fr/course/view.php?id=407#section-11>
(Please use only as a guidance)

- ◆ What molecular modeling method was used and why?
- ◆ Was it a fully atomistic simulations, or some simplified models were used?
- ◆ What other approximations were used in the modeling?
- ◆ What was the number of particles in the simulations? Was it big enough for the specific problem? Was it small enough to make the simulations computationally efficient?
- ◆ How long-range electrostatic interactions were handled in the simulations? Was it important for the given problem?
- ◆ What kind of boundary conditions were applied to the simulation box? Why?
- ◆ What properties of the system were calculated from the molecular simulation?
- ◆ Make a qualitative assessment of the accuracy for the calculated properties given the number of atoms in the simulated system and the duration of the simulation.
- ◆ What other properties would you additionally calculate from the same simulations for the same system?
- ◆ Formulate 2 or 3 strong points of the given molecular simulation paper and 2 or 3 weak points of the paper.